# Cis binding between inhibitory receptors and MHC class I can regulate mast cell activation

**Ai Masuda, Akira Nakamura, Tsutomu Maeda, Yuzuru Sakamoto, and Toshiyuki Takai**

Department of Experimental Immunology and Core Research for Evolutional Science and Technology, Japan Science and Technology Agency, Institute of Development, Aging and Cancer, Tohoku University, Aoba-ku, Sendai-shi 980-8575, Japan

**Allergy is caused by immune effector cells, including mast cells and basophils. Cellular signaling that activates these effector cells is regulated by different inhibitory receptors on their surface. We show that human leukocyte immunoglobulin (Ig)-like receptor (LILR) B2 and its mouse orthologue, paired Ig-like receptor (PIR)–B, constitutively associate to major histocompatibility complex (MHC) class I on the same cell surface (in cis). The IgE-mediated effector responses were augmented in $\beta_2$-microglobulin ($\beta_2$m) and PIR-B–deficient mast cells. In addition, the increased cytokine production of $\beta_2$m-deficient mast cells was not affected by the co-culture with MHC class I–positive mast cells, showing that less cis interaction between PIR-B and MHC class I on mast cells led to the increased cytokine release. Thus, the constitutive cis binding between LILRB2 or PIR-B and MHC class I has an essential role in regulating allergic responses.**

CORRESPONDENCE
Toshiyuki Takai:
tostakai@idac.tohoku.ac.jp

Abbreviations used: BMMC, bone marrow–derived mast cell; $\beta_2$m, $\beta_2$-microglobulin; FcεRI, high affinity FcR for IgE; FcγRIIB and FcγRIII, type IIB and type III, respectively, low affinity FcR for IgG; FRET, fluorescence resonance energy transfer; HRP, horseradish peroxidase; ITAM, immunoreceptor tyrosine–based activation motif; ITIM, immunoreceptor tyrosine–based inhibition motif; LILR, leukocyte Ig-like receptor; MIP, macrophage inflammatory protein; PIR, paired Ig-like receptor; PLC, phospholipase C; PMT, photomultiplier; SHP, Src homology domain 2–containing tyrosine phosphate; SIRP, signal regulatory protein.

Mast cells and basophils, which are derived from hematopoietic progenitor cells, are key effector cells in IgE-mediated immune responses, such as allergy and host protection against parasites (1–4). Upon binding of the antigen to IgE, these effector cells immediately release various proinflammatory molecules, including chemical mediators and cytokines (1–4). These cells express high affinity FcR for IgE (FcεRI), which is composed of an IgE-binding α subunit, a β subunit (FcεRIβ), and a disulphide-bonded γ subunit (FcRγ) homodimer (4, 5). Both FcRγ and FcεRIβ contain a cytoplasmic amino acid sequence termed immunoreceptor tyrosine–based activation motif (ITAM) (4, 5). Upon clustering of FcεRI by IgE and multivalent antigens, the intracellular Src family protein tyrosine kinases phosphorylate tyrosine residues of the ITAMs of FcRγ and FcεRIβ (4, 5). The phosphorylated ITAM serves as the binding site for Syk, resulting in its activation and autophosphorylation, which leads to the induction of a further downstream signaling cascade (4). Mast cells and basophils also express other ITAM-bearing receptors, such as type III low affinity FcR for IgG (FcγRIII), and many activating-type receptors, including Toll-like receptors, as well as those for complement components like cytokines and chemokines (2, 3). These receptors can also activate mast cells or basophils upon binding to their cognate ligands, resulting in the de novo synthesis and release of cytokines, chemokines, and lipid mediators (1–4). Upon stimulation by these activating receptors, mast cells or basophils are triggered within a few minutes, thus leading to acute hypersensitive responses, such as anaphylaxis and acute asthma attack (4). Moreover, the constitutive binding of monomeric IgE molecules to FcεRI can amplify cell-surface expression of FcεRI and its signaling (1, 4, 6).

Considering the presence of different ways to stimulate mast cell or basophil activation cascades, one may predict the importance of the counterregulatory system of mast cells or basophils, which tightly suppress any spontaneous or excessive activation of the cells. In fact, like other cells in the immune system, mast cells and basophils express various inhibitory receptors, which counteract activating receptors on the same cells (7). In mice, these include FcγRIIB (7, 8), mast cell function–associated antigen (9), and gp49B (10), all of which harbor one or more immunoreceptor tyrosine–based inhibitory motifs (ITIMs) in their cytoplasmic

A. Masuda and A. Nakamura contributed equally to this work.

portions. When coengaged with activating-type receptors such as FcεRI, the tyrosine residues in these ITIMs of the inhibitory receptors are phosphorylated (1, 7) and recruit Src homology domain 2–containing inositol polyphosphate 5′-phosphatase (1, 7) or Src homology domain 2–containing tyrosine phosphate (SHP)–1 (1, 7), both of which dephosphorylate the ITAM-induced signaling molecules. Therefore, mast cells lacking these inhibitory receptors are sensitive to IgE stimulation (7). In contrast, mast cells lacking activating receptors show attenuated responses to various stimulation, indicating that the mast cell activation is regulated by adequate balancing between activating and inhibitory receptors (1–4, 7).

Leukocyte Ig-like receptors (LILRs) are a family of Ig-like receptors encoded by several genes and are expressed on various immune cells, such as those of myeloid and lymphoid lineages (11, 12). LILRs are divided into two types of receptors: activating-type receptors (LILRA1–A6) and inhibitory-type receptors (LILRB1–B5). Activating-type LILRs, which associate with FcRγ, deliver positive signals into the cells, whereas inhibitory-type LILRs harbor ITIMs in their cytoplasmic portions and deliver inhibitory signaling by recruiting SHP-1 to the phosphotyrosylated ITIMs (11, 12). Although it remains unclear whether LILRs are expressed on mast cells, peripheral basophils express several LILRs, such as LILRA2, LILRB2, and LILRB3 proteins (13). Recent studies demonstrated that LILRA2 can elicit effector functions of basophils upon cross-linking with antibodies (13). Moreover, LILRB2 represses the basophil activation stimulated with IgE or anti-LILRA2 (13), showing that LILRs have an essential role in the function of basophils. Although a full spectrum of the ligands for LILRs is not yet clarified, several LILRs are found to recognize MHC class I molecules as their ligands (12, 14). In particular, LILRB1 and LILRB2 can bind various classical or nonclassical MHC class I without allele specificity (14).

Mouse LILR relatives or orthologues, paired Ig-like receptors (PIRs) (15, 16) are also composed of two isoforms, activating PIR-A and inhibitory PIR-B, expressed on various hematopoietic cell lineages, including B cells, mast cells, macrophages, granulocytes, and DCs, but are not expressed on T cells and NK cells (16, 17). PIR-A requires ITAM-containing FcRγ for its cell-surface expression and signal transduction (17–21). In contrast, PIR-B contains ITIMs in its cytoplasmic portion and inhibits activation signaling upon coengagement with other activating receptors (20, 22, 23). Indeed, artificial cross-linking of PIR-B to FcεRI-bound IgE with antibodies suppressed the IgE-mediated calcium response and degranulation of mast cells, suggesting that PIR-B can suppress FcεRI-mediated mast cell signaling (24).

Recently, we found that PIR-B, as well as PIR-A, can bind MHC class I molecules (25). Like LILRB1 and LILRB2 proteins, the recombinant PIR-B had similar binding affinities to various mouse MHC class I proteins. Therefore, the identification of the ubiquitously expressed "self" marker proteins as the ligands for PIRs and LILRs raises the possibility of whether cells expressing PIRs or LILRs, such as mast cells and basophils, could be autoregulated by the MHC class I molecules expressed on their own (in cis) or influenced by the self-marker molecules on the surrounding cells (in trans), or both. Clarifying this question should be fundamentally important, because it will provide us with an invaluable notion of the mode of regulation in MHC class I and its receptors, which probably constitute pivotal components maintaining peripheral tolerance. As predicted by the missing-self hypothesis (26), various inhibitory receptors for MHC class I molecules have been identified in NK cells and T cell subsets (27–29), such as killer Ig-like receptors (30), CD94/NKG2A heterodimers (31), and the C-type lectin superfamily, including mouse Ly49 receptors (32). In the NK cell case, trans regulation has been verified to be important, because MHC class I on surrounding cells is monitored through their inhibitory MHC class I receptors that suppress NK cell–mediated cytotoxicity against class I–bearing normal cells and target abnormal cells that do not sufficiently express MHC class I, such as virus-infected cells (27, 29). Recent analysis on mouse Ly49A suggested the consequences of both cis and trans interactions between Ly49A and its ligand H-2D$^d$ for the optimal regulation of NK cells (33). However, little is known about the mode of regulation for other MHC class I–recognizing receptors such as LILRs on other immune cells, including basophils. In particular, mechanisms of PIRs and the MHC class I binding in mast cell regulation remain to be clarified, although the possible significance of PIR-B in allergic reactions has been suggested, because Th2 cell–skewed immune responses, in terms of increased IL-4 production and enhanced IgG1 and IgE production, were seen in PIR-B–deficient (*Pirb*$^{-/-}$) mice in response to immunization with thymus-dependent antigens (34).

In this paper, we demonstrate the physiologic importance of constitutive cis association between LILRB2 or PIR-B and MHC class I on human basophilic cell lines or mouse mast cells, respectively. In particular, mast cells from either *Pirb*$^{-/-}$ mice or MHC class I–deficient $\beta_2$-microglobulin ($\beta_2$m)–deficient (*B2m*$^{-/-}$) mice and these animals themselves revealed similar profiles upon stimulation, namely IgE- and FcεRI-mediated degranulation, cytokine and lipid mediator release, and systemic anaphylaxis. These results show the essential role of the self-recognizing PIR-B or LILRB2 system in the suppression of allergic responses.

## RESULTS

### Cis association between LILRB2 and MHC class I

We initially examined cell-surface expression of inhibitory LILRs on human basophilic KU812 cells by flow cytometry. Consistent with the published data of human peripheral basophils (13), KU812 cells express LILRB2 and LILRB3 but not LILRB1 and LILRB4 (Fig. 1 A). KU812 cells also express substantial levels of FcεRI, HLA-A, B, C, and $\beta_2$m (Fig. 1 B).

LILRB2s are known to recognize a broad range of classical MHC class I molecules and nonclassical MHC class I

molecules, such as HLA-G (14). However, the cell-surface localization of LILRB2 and MHC class I remains to be clarified. Therefore, we next investigated LILRB2 and HLA-A, B, C expression on KU812 cells by confocal microscopy. LILRB2 was clearly colocalized within a pixel (~20 nm) with HLA-A, B, C on the same cell surface as KU812 cells (Fig. 1 B). On the other hand, unlike LILRB2, LILRB3 does not bind MHC class I (14); thus, we used it as the

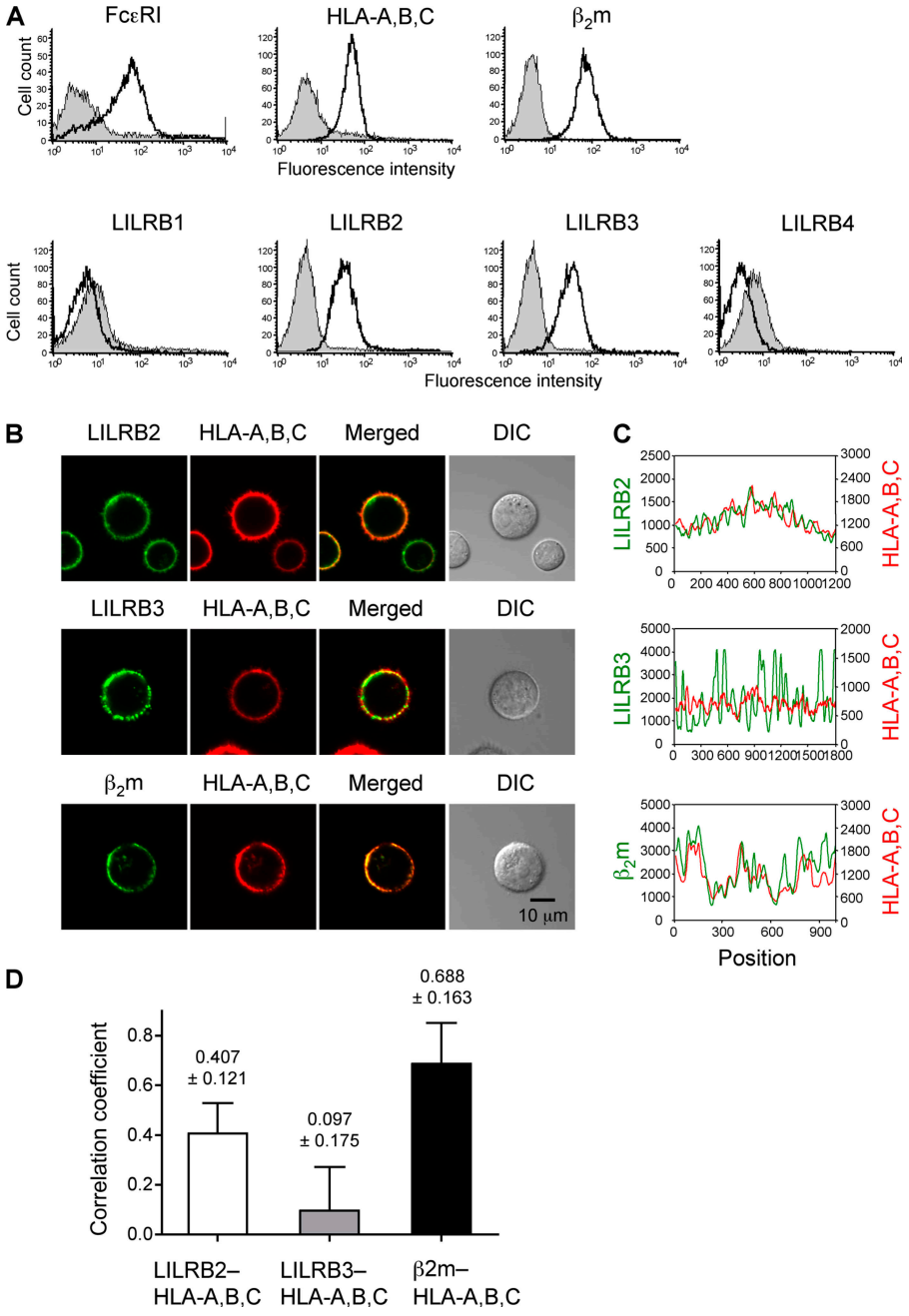


**Figure 1. Expression of LILRs on KU812 cells.** (A) Flow cytometric analysis of cell-surface expression on KU812 cells stained with mAb against FcεRI (CRA1), HLA-A, B, C (G46-2.6), $\beta_2$m (TÜ99), LILRB1 (GHI/75), LILRB2 (287219), LILRB3 (222821), and LILRB4 (ZM3.8). (B) Confocal imaging of KU812 cells. KU812 cells were stained with (top) Alexa Fluor 546–conjugated anti-LILRB2 (287219) and Alexa Fluor 647–conjugated anti–HLA-A, B, C (G46-2,6), (middle) Alexa Fluor 546–conjugated anti-LILRB3 (222821) and Alexa Fluor 647–conjugated anti–HLA-A, B, C, and (bottom) Alexa Fluor 546–conjugated anti-$\beta_2$m (TÜ99) and Alexa Fluor 647–conjugated anti–HLA-A, B, C. DIC, differential interference contrast. (C) The fluorescence profile histogram for each image demonstrated the relative fluorescence intensity in each pixel (y axis) along the linearized cell surface (x axis). (D) Correlation coefficients calculated for colocalization of LILRB2, LILRB3, $\beta_2$m, and HLA-A, B, C in KU812 cells are shown ($n = 15$). Data are shown as mean ± SD.

negative control. Indeed, LILRB3 did not overlap with HLA-A, B, C (Fig. 1 B). To further quantitatively confirm the colocalization between LILRB2 and HLA-A, B, C, the fluorescence intensity values were measured. As shown in Fig. 1 C, illustrating the linearized fluorescence intensity profiles, the colocalization between LILRB2 and HLA-A, B, C was much more substantial than that between LILRB3 and HLA-A, B, C. In addition, the correlation coefficient ($\sigma_{x,y}$) was calculated for the intensity between LILRB2 or LILRB3 and HLA-A, B, C. The $\sigma_{x,y}$ between LILRB2 and HLA-A, B, C ($\sigma_{x,y}$ = 0.407 ± 0.121) was considerably higher than that between LILRB3 and HLA-A, B, C ($\sigma_{x,y}$ = 0.097 ± 0.175; Fig. 1 D). As a positive control, $\beta_2$m was colocalized well with HLA-A, B, C ($\sigma_{x,y}$ = 0.688 ± 0.163; Fig. 1, B–D). These results suggested that LILRB2 can bind MHC class I on the same cell surface in cis.

To confirm the cis association between LILRB2 and MHC class I on KU812 cells, we also performed fluorescence resonance energy transfer (FRET) analysis by confocal laser microscopy with Alexa Fluor 546–conjugated anti-LILRB2 mAb as an energy donor and Alexa Fluor 647–conjugated anti-HLA-A, B, C mAb as an acceptor, because the efficiency of the FRET from donor to acceptor represents a very sensitive indicator of the molecular colocalization on a scale of 2–10 nm (Fig. 2) (35). Table I summarizes the FRET efficiencies between donors and acceptors obtained by the confocal laser microscopy. When KU812 cells were doubly stained with Alexa Fluor 546–conjugated LILRB2 mAb (green) and Alexa Fluor 647–conjugated HLA-A, B, C mAb (red) and then excited with the 543-nm laser, we detected a strong FRET effect from the excited LILRB2 mAb signal to the HLA-A, B, C mAb signal (20.7 ± 3%; Fig. 2 and Table I). As a positive control, $\beta_2$m showed a strong energy transfer with HLA-A, B, C (14.5 ± 4.7%; Fig. 2 and Table I). In contrast, negative control LILRB3 did not show a notable energy transfer with HLA-A, B, C on KU812 cells (4 ± 4.9%; Fig. 2 and Table I). These findings demonstrate that LILRB2 can associate with MHC class I in cis.

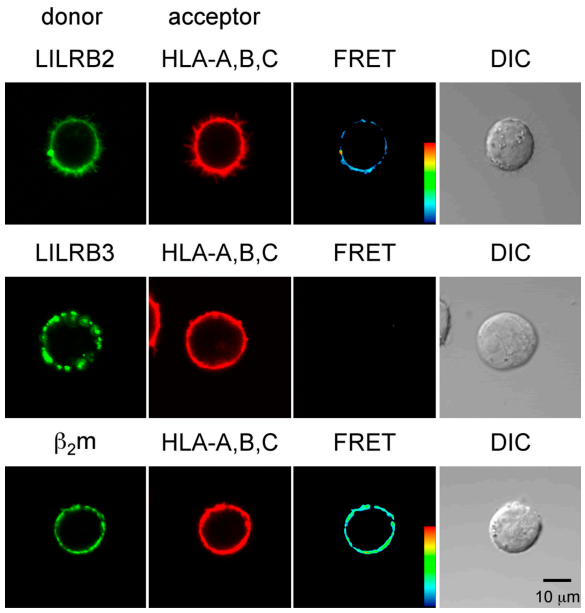


**Figure 2. Cis association between LILRB2 and MHC class I on KU812 cells.** Colocalization of LILRB2 and HLA-A, B, C by FRET analysis is shown. From left to right, excited donor (Alexa Fluor 546–conjugated LILIRB2 mAb [287219], LILRB3 [222821], and $\beta_2$m mAb [TÜ99]) images (green), excited acceptor (Alexa Fluor 546–conjugated HLA-A, B, C [G46-2.6]) images (red), FRET signal images (pseudocolor), and DIC images are shown. The cis association between LILRB2 or $\beta_2$m and HLA-A, B, C was determined by FRET. DIC, differential interference contrast.

**Table I.** FRET efficiency between donor/acceptor pairs bound to LILRB2, LILRB3, and $\beta_2$m on KU812 cells

| FRET pairs | | FRET efficiency (%)[a] |
|---|---|---|
| Donor antibody (Alexa Fluor 546) | Acceptor antibody (Alexa Fluor 647) | |
| LILRB2 | HLA-A, B, C | 20.7 ± 3 |
| LILRB3 | HLA-A, B, C | 4 ± 4.9 |
| $\beta_2$m | HLA-A, B, C | 14.5 ± 4.7 |

Energy transfer between different pairs was detected from the increase in donor fluorescence after acceptor photobleaching. FRET efficiency (%) = (1 − fluorescence intensity of prebleach donor cells/fluorescence intensity of postbleach donor cells) × 100. FRET efficiency >5 was defined as the threshold level for substantial transfer efficiency.
[a]Data are the mean ± SD ($n$ = 15).

### Cis association between PIR-B and MHC class I

To investigate the detailed function of the inhibitory receptor for MHC class I in vitro or in vivo, we next investigated the physiological role of mouse LILRB2/B3 relatives, PIR-B, and MHC class I on bone marrow–derived mast cells (BMMCs) from C57BL/6 (B6), *B2m*$^{-/-}$, or *Pirb*$^{-/-}$ mice induced by the IL-3–conditioned medium (36). In initial studies, we confirmed comparable expression levels of FcεRI, c-Kit, and IL-3 receptor α chain on *B2m*$^{-/-}$ or *Pirb*$^{-/-}$ BMMCs by flow cytometry (Fig. 3 A). *B2m*$^{-/-}$ BMMCs also showed an expression level of PIR-A/B comparable to that of B6 BMMCs (Fig. 3 A), whereas *Pirb*$^{-/-}$ BMMCs showed a very low level of PIR-A expression, indicating a dominant expression of PIR-B on mast cells, as previously indicated (24, 34). Regarding MHC class I expression, the staining of B6 or *Pirb*$^{-/-}$ BMMCs with H-2K$^b$/D$^b$ mAb yielded comparable expression levels of these MHC class I molecules (Fig. 3 A). A very low level of H-2D$^b$ expression on *B2m*$^{-/-}$ BMMCs detected with anti-H-2D$^b$ mAb (Fig. 3 A) may indicate an expression of the H-2 heavy chain dimer, because the mAb is able to bind both the canonical H-2 heavy chain/$\beta_2$m heterodimeric structure and the $\beta_2$m-less heavy chain homodimeric structure (37, 38).

Because LILRB2 associates with MHC class I on human basophilic KU812 cells in cis, we also explored the localization of PIRs and MHC class I on mouse mast cells by confocal microscopy. PIR-A/B was colocalized with H-2D$^b$ on the same cell surface of B6 BMMCs (Fig. 3 B). A weak but definite colocalization of PIR-A and MHC class I on *Pirb*$^{-/-}$

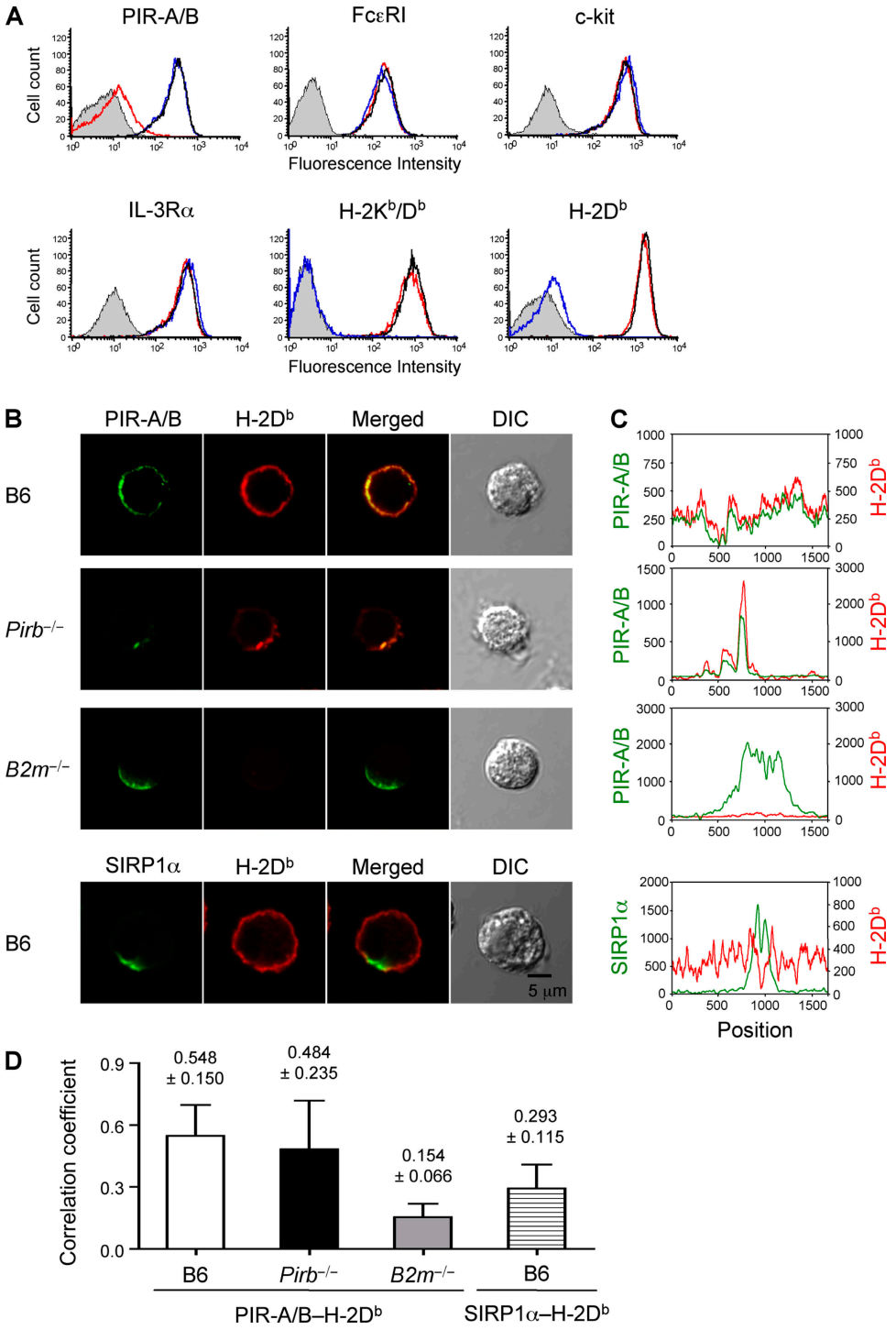


**Figure 3. Expression of PIR-A/B and MHC class I on mast cells.** (A) Flow cytometric analysis of cell-surface expression on BMMCs. After a 1-h incubation with anti-TNP-IgE, BMMCs from B6 (black line), *Pirb*$^{-/-}$ (red line), or *B2m*$^{-/-}$ (blue line) mice were stained with anti–PIR-A/B (6C1), anti-IgE (R35-72), anti–c-Kit (2B8), anti–IL-3Rα (5B11), H-2K$^b$/D$^b$ (28-8-6), and H-2D$^b$ (B22-249.R1). Isotype control stainings (rat IgG1κ [R3-34]) or rat IgG2a [R35-95]) are shown (shaded area). (B) Confocal imaging of BMMCs. (top) B6, *Pirb*$^{-/-}$, or *B2m*$^{-/-}$ BMMCs were stained with Alexa Fluor 488–conjugated anti–PIR-A/B (6C1) and Alexa Fluor 546–conjugated anti–H-2D$^b$ (28-17-8). (bottom) B6 BMMCs were stained with Alexa Fluor 488–conjugated SIRP1α (P84) and Alexa Fluor 546–conjugated anti–H-2D$^b$ (28-17-8). DIC, differential interference contrast. (C) Relative fluorescence intensity of the linearized cell surface in each individual cell is shown. (D) Correlation coefficients calculated for the colocalization of PIR-A/B, SIRP1α, and H-2D$^b$ are shown ($n = 15$). Data are shown as mean ± SD.

BMMCs was also detected (Fig. 3 B). Our fluorescent microscopy failed to detect any robust signal for H-2D$^b$ on *B2m*$^{-/-}$ BMMCs (Fig. 3 B). The linearization of the fluorescence intensity and the $\sigma_{x,y}$ between PIR-B and H-2D$^b$ ($\sigma_{x,y}$ = 0.548 ± 0.15) clearly showed the colocalization between PIR-B and H-2D$^b$ on the same cell surface (Fig. 3, C and D). Moreover, the linearization of the fluorescence intensity and the $\sigma_{x,y}$ between PIR-A and H-2D$^b$ ($\sigma_{x,y}$ = 0.484 ± 0.235) also showed the colocalization between PIR-A and H-2D$^b$ on the same cell surface of *Pirb*$^{-/-}$ BMMCs (Fig. 3, C and D). As a negative control, the fluorescence of signal regulatory protein (SIRP) 1α (39), an inhibitory Ig-like receptor that recognizes integrin-associated protein CD47, did not overlap with that of MHC class I (Fig. 3, B–D). These findings strongly suggest that PIR-A/B can also bind MHC class I in cis.

To further confirm the cis association between PIR-B and MHC class I on BMMCs, we also performed FRET analysis with Alexa Fluor 546–conjugated anti–PIR-A/B mAb as an energy donor and Alexa Fluor 647–conjugated anti–H-2D$^b$ mAb as an acceptor (Fig. 4). Table II summarizes the FRET efficiencies between donor–acceptor pairs bound to PIR-A/B, H-2K$^b$/D$^b$, and SIRP1α. When B6 BMMCs were doubly stained with Alexa Fluor 546–conjugated PIR-A/B mAb (green) and Alexa Fluor 647–conjugated H-2K$^b$/D$^b$ mAb (red) and excited with the 543-nm laser, we detected a strong FRET effect from the excited PIR-A/B mAb signal to the H-2K$^b$/D$^b$ mAb signal (13.5 ± 9.8%; Fig. 4 and Table II). A positive control, $\beta_2$m showed a substantial energy transfer with H-2K$^b$/D$^b$ (8 ± 3.1%; Fig. 4 and Table II). However, we failed to detect any substantial FRET effect between PIR-A and H-2K$^b$/D$^b$ on *Pirb*$^{-/-}$ BMMCs (Fig. 4 and Table II). A negative control SIRP1α showed no energy transfer with H-2D$^b$ (Fig. 4 and Table II). These findings demonstrate that PIR-B, as well as LILRB2, can associate with MHC class I in cis.

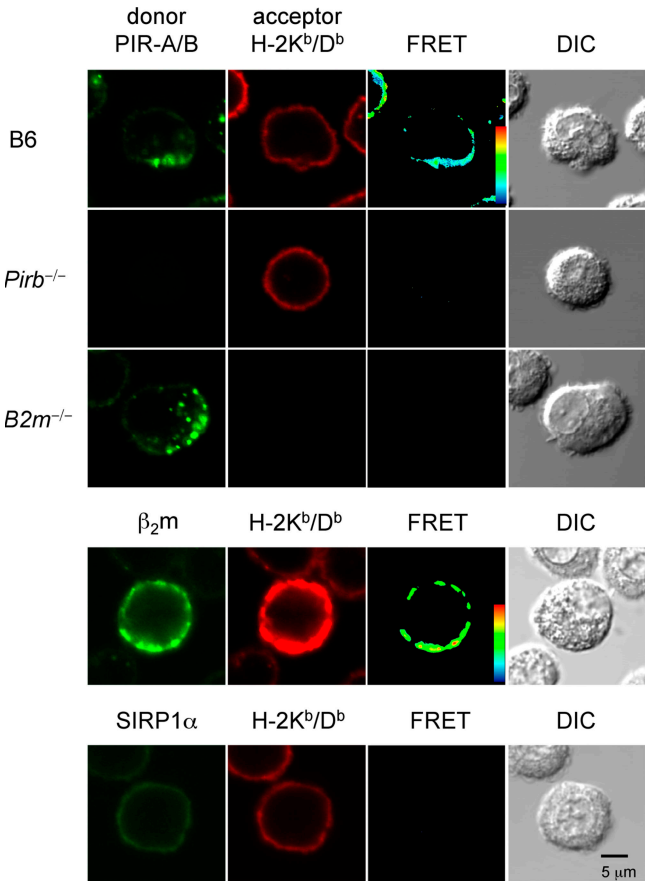


**Figure 4. Cis association between PIR-B and MHC class I on mast cells.** Colocalization of PIR-B and H-2K$^b$/D$^b$ by FRET analysis. From left to right, excited donor (Alexa Fluor 546–conjugated PIR-A/B mAb [6C1], $\beta_2$m mAb [S19.8], and SIRP1α mAb [P84]) images (green), excited acceptor (Alexa Fluor 647–conjugated H-2K$^b$/D$^b$ [28-8-6]) images (red), FRET signal images (pseudocolor), and DIC images are shown. The cis association between PIR-B or $\beta_2$m and H-2K$^b$/D$^b$ was determined by FRET. DIC, differential interference contrast.

### *B2m*$^{-/-}$ or *Pirb*$^{-/-}$ BMMCs are hypersensitive to IgE or LPS stimulation

Engagement of FcεRI on mast cells with IgE and multivalent antigens leads to degranulation and cytokine responses (1–5). To clarify whether the association between PIR-B and MHC class I physiologically regulates IgE-mediated mast cell activation, BMMCs were stimulated with TNP-OVA after sensitization with IgE specific for TNP. The degranulation responses were measured by histamine ELISA. Both *B2m*$^{-/-}$ and *Pirb*$^{-/-}$ BMMCs showed an augmented release of histamine compared with B6 BMMCs (Fig. 5 A), indicating a suppressive role of either MHC class I or PIR-B on mast cell degranulation. We also examined cytokine and chemokine production after cross-linking of FcεRI. Consistent with the results of histamine ELISA, both *B2m*$^{-/-}$ and *Pirb*$^{-/-}$ BMMCs produced more IL-1β, GM-CSF, and macrophage inflammatory protein (MIP)–1α than B6 BMMCs (Fig. 5 B).

**Table II.** FRET efficiency between donor/acceptor pairs bound to PIR-A/B, H-2K$^b$/D$^b$, and SIRP1α on BMMCs from B6, *B2m*$^{-/-}$, or *Pirb*$^{-/-}$ mice

| Mice | FRET pairs | | FRET efficiency (%)[a] |
|---|---|---|---|
| | Donor antibody (Alexa Fluor 546) | Acceptor antibody (Alexa Fluor 647) | |
| B6 | PIR-A/B | H-2K$^b$/D$^b$ | 13.5 ± 9.8 |
| *B2m*$^{-/-}$ | PIR-A/B | H-2K$^b$/D$^b$ | n.d. |
| *Pirb*$^{-/-}$ | PIR-A/B | H-2K$^b$/D$^b$ | 3.9 ± 3.7 |
| B6 | H-2K$^b$/D$^b$ | $\beta_2$m | 8 ± 3.1 |
| B6 | SIRP1α | H-2K$^b$/D$^b$ | n.d. |

Energy transfer between different pairs was detected from the increase in donor fluorescence after acceptor photobleaching. FRET efficiency (%) = (1 − fluorescence intensity of prebleach donor cells/fluorescence intensity of postbleach donor cells) × 100. FRET efficiency >5 was defined as the threshold level for substantial transfer efficiency. n.d., not detected (FRET efficiency < 0%).
[a]Data are the mean ± SD ($n$ = 15).

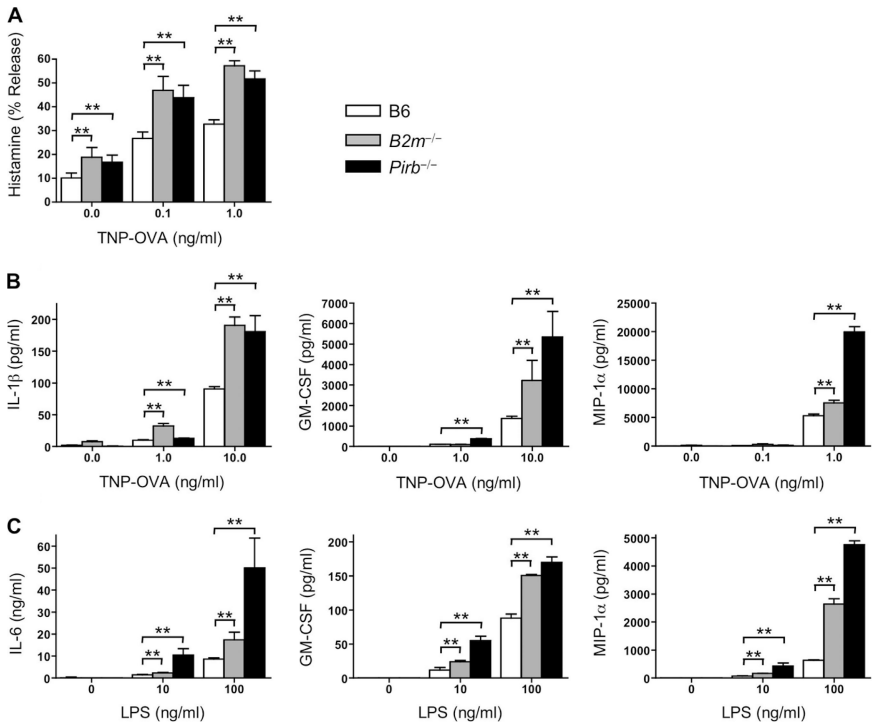


**Figure 5. Enhanced histamine, cytokine, and chemokine production in *B2m*$^{-/-}$ or *Pirb*$^{-/-}$ BMMCs stimulated with IgE or LPS.** (A and B) B6, *B2m*$^{-/-}$, or *Pirb*$^{-/-}$ BMMCs were incubated with TNP-OVA for 12 h at the indicated concentrations 1h after sensitization with 5 μg/ml anti-TNP-IgE. (A) The percentage of histamine release by BMMCs was determined by ELISA ($n = 3$). (B) Concentration of IL-1β, GM-CSF, and MIP-1α in the culture media was measured by ELISA ($n = 3$). (C) B6, *B2m*$^{-/-}$, or *Pirb*$^{-/-}$ BMMCs were incubated with LPS for 12 h at the indicated concentrations. Concentrations of IL-6, GM-CSF, and MIP-1α in the culture media were measured by ELISA ($n = 3$). Data are shown as mean ± SD of the average of the three different BMMC cultures. Statistical analyses were performed using the Student's *t* test. **, $P < 0.01$ between *B2m*$^{-/-}$ or *Pirb*$^{-/-}$ and B6 BMMCs.

These results suggested that the interaction between PIR-B and MHC class I is physiologically critical to regulate the mast cell activation triggered by IgE. On the other hand, mast cells express various activating-type receptors other than FcεRI. To evaluate whether the deletion of PIR-B or MHC class I effects the mast cell activation triggered by other activating-type receptors, we next investigated cytokine production after stimulation with LPS. As shown in Fig. 5 C, both *B2m*$^{-/-}$ and *Pirb*$^{-/-}$ BMMCs produced more IL-6, GM-CSF, and MIP-1α than B6 BMMCs. These results suggested that the association between PIR-B and MHC class I inhibits LPS-mediated mast cell activation and also suggested that the PIR-B–MHC class I inhibitory system can maintain the activation threshold of the mast cell stimulated with various activation-type receptors.

### Cis interaction between PIR-B and MHC class I regulates mast cell activation

In in vitro culture, mast cells could interact with each other, and, thus, PIR-B might also bind MHC class I on surrounding mast cells (trans interaction). Therefore, to evaluate whether PIR-B associates with MHC class I in cis or trans, or both, *B2m*$^{-/-}$ BMMCs were co-cultured with *Pirb*$^{-/-}$ or B6 BMMCs at a 1:1 ratio, because PIR-B on *B2m*$^{-/-}$ BMMCs can interact with MHC class I in trans only. After IgE stimulation, IL-6 production was measured by ELISA. If PIR-B binds MHC class I in trans, IL-6 production from *B2m*$^{-/-}$ BMMCs mixed with *Pirb*$^{-/-}$ or B6 BMMCs would decrease because of the inhibitory signaling by PIR-B. Consistent with the observation in Fig. 5, both *B2m*$^{-/-}$ and *Pirb*$^{-/-}$ BMMCs produced more IL-6 than B6 BMMCs (Fig. 6, gray-shaded and black-shaded columns vs. open column). In particular, *Pirb*$^{-/-}$ BMMCs produced higher levels of IL-6 than *B2m*$^{-/-}$ BMMCs (black-shaded vs. gray-shaded column). On the other hand, *B2m*$^{-/-}$ BMMCs mixed with *Pirb*$^{-/-}$ BMMCs produced an almost similar level of IL-6 compared with *Pirb*$^{-/-}$ BMMCs alone (diagonally hatched column vs. black-shaded column), showing that the cytokine production of *B2m*$^{-/-}$ BMMCs is not affected by the co-culture with MHC class I–positive mast cells. These results indicated that PIR-B on BMMCs predominantly associates with MHC class I in cis, thereby regulating mast cell activation in vitro.

### Augmented FcεRI-mediated signal transduction in *B2m*$^{-/-}$ or *Pirb*$^{-/-}$ BMMCs

To further investigate the regulatory effect of the cis association between PIR-B and MHC class I, FcεRI-mediated

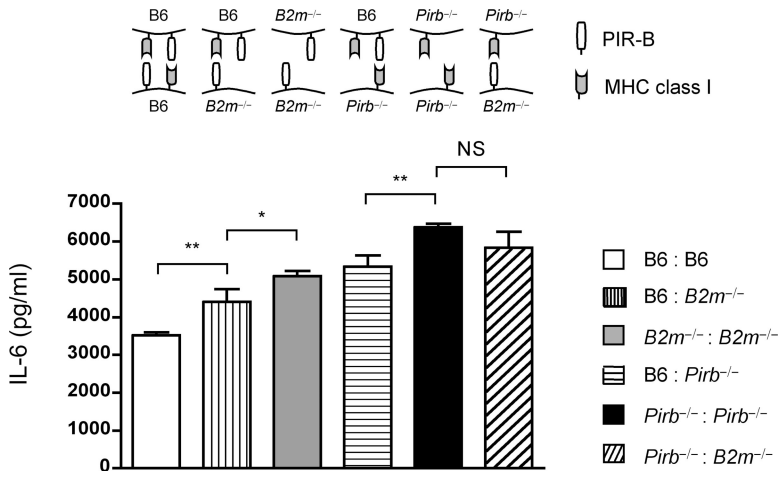


**Figure 6. PIR-B on BMMCs associates with MHC class I in cis.** $2 \times 10^6$ B6, $B2m^{-/-}$, or $Pirb^{-/-}$ BMMCs were mixed with each other for 12 h at a 1:1 ratio. Mixed BMMCs were incubated with 10 ng/ml TNP-OVA for 12 h after sensitization with 5 μg/ml anti-TNP-IgE. The concentration of IL-6 in the culture media was determined by ELISA ($n = 3$). Data are shown as mean ± SD of the average of the three different BMMC cultures. (top) Diagrams show the BMMC combination corresponding to each column. Statistical analyses were performed using the Student's *t* test. **, $P < 0.01$ between the indicated mixed BMMC lines.

signaling was investigated in either $B2m^{-/-}$ or $Pirb^{-/-}$ BMMCs. We first examined the tyrosine phosphorylation status of PIR-B in B6 and $B2m^{-/-}$ BMMCs after stimulation with IgE and TNP-OVA. As shown in Fig. 7 A, PIR-B was constitutively phosphorylated in B6 BMMCs without any stimulation. Upon clustering of FcεRI with IgE and TNP-OVA, the PIR-B tyrosine phosphorylation immediately increased (Fig. 7, A and B). In contrast, the PIR-B phosphorylation was significantly reduced in resting as well as in stimulated $B2m^{-/-}$ BMMCs, showing that the absence of cis interaction of PIR-B with MHC class I diminished the constitutive as well as the induced PIR-B phosphorylation (Fig. 7, A and B). Consistent with the reduced phosphorylation, PIR-B in $B2m^{-/-}$ BMMCs also showed a decreased SHP-1 recruitment (Fig. 7, A and B). Concomitant with either the reduction of the inhibitory signaling through PIR-B in $B2m^{-/-}$ BMMCs or the complete loss of PIR-B–mediated inhibition in $Pirb^{-/-}$ cells, FcεRI-mediated phospholipase C (PLC)–γ2 phosphorylation was remarkably enhanced (Fig. 7, A and B). In addition, the phosphorylation status of FcRγ, which associates with FcεRI and PIR-A, was augmented in $B2m^{-/-}$ and in $Pirb^{-/-}$ BMMCs (Fig. 7, A and B). The $Ca^{2+}$ mobilization after stimulation with IgE and TNP-OVA was also substantially enhanced in $B2m^{-/-}$ as well as in $Pirb^{-/-}$ BMMCs (Fig. 7 C). These findings showed that the PIR-B–MHC class I interaction in cis is critical for the inhibitory signaling against the stimulation through FcεRI.

### IgE-dependent passive systemic anaphylaxis is enhanced either in $B2m^{-/-}$ or $Pirb^{-/-}$ mice

To verify whether the deletion of PIR-B or MHC class I impairs the mast cell activation in vivo, IgE-mediated passive systemic anaphylaxis was induced in $B2m^{-/-}$ or $Pirb^{-/-}$ mice. This assay reflects in vivo IgE-mediated mast cell activation (7). Mice were first intravenously injected with monoclonal anti-TNP IgE, followed by a challenge with TNP-OVA 24 h after injection. After administration with TNP-OVA, the rectal temperature was monitored. Upon FcεRI cross-linking, either $B2m^{-/-}$ or $Pirb^{-/-}$ mice showed a significant decrease in rectal temperature compared with that of B6 mice (Fig. 8 A). Histopathological findings of ear sections also showed augmented degranulation of mast cells in either $B2m^{-/-}$ or $Pirb^{-/-}$ mice (Fig. 8, B and C). These results were consistent with the in vitro studies on mast cells and suggested that the PIR-B–MHC class I interaction inhibits in vivo mast cell activation. On the other hand, we also induced anaphylaxis in FcγRIIB-deficient ($Fcgr2b^{-/-}$) mice under the same condition. $Fcgr2b^{-/-}$ mice showed a more severe anaphylactic response than $Pirb^{-/-}$ mice (unpublished data), suggesting that FcγRIIB strongly regulates IgE-mediated mast cell activation more than other inhibitory receptors, including PIR-B, because FcγRIIB can directly bind to IgE as well as IgG (40). Finally, to investigate whether PIR-B regulates the mast cell activation through the interaction with MHC class I in trans in vivo, we induced anaphylaxis in mast cell–deficient WBB6$F_1$-$Kit^W/Kit^{W\text{-}v}$ ($W/W^v$) mice reconstituted with B6, $B2m^{-/-}$, or $Pirb^{-/-}$ BMMCs. However, as shown in Fig. 8 D, the passive anaphylaxis was not induced in $W/W^v$ mice reconstituted with $B2m^{-/-}$ BMMCs because of the failure of the reconstitution (not depicted). It is possible that other immune cells, such as NK cells, eliminated the transferred $B2m^{-/-}$ BMMCs. In contrast, $W/W^v$ mice reconstituted with $Pirb^{-/-}$ BMMCs showed an augmented anaphylactic response compared with $W/W^v$ mice reconstituted with B6 BMMCs. Thus, further analysis would be required to distinguish the contributions of cis and trans

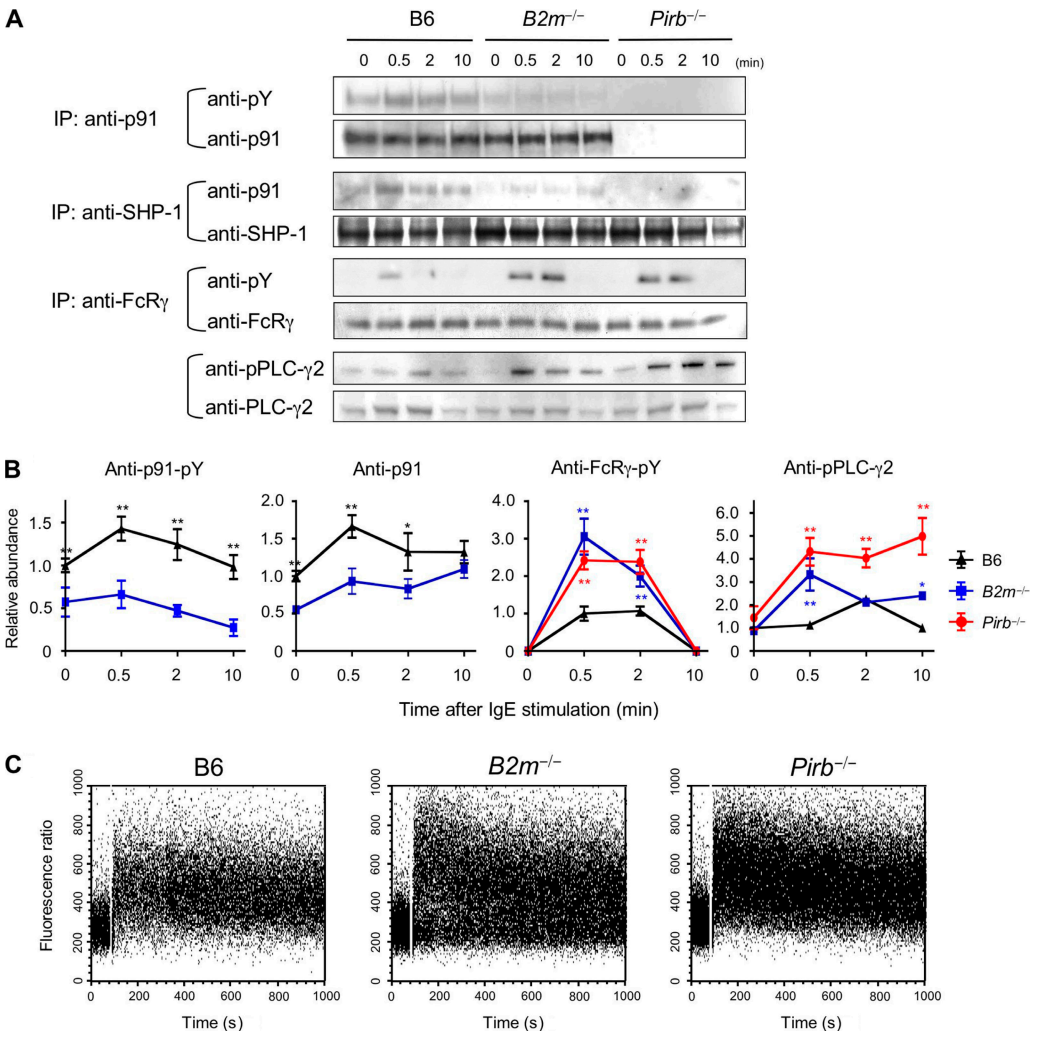


**Figure 7. Augmented intracellular signaling in *B2m*$^{-/-}$ or *Pirb*$^{-/-}$ BMMCs stimulated with IgE.** (A) B6, *B2m*$^{-/-}$, or *Pirb*$^{-/-}$ BMMCs were stimulated with 10 ng/ml TNP-OVA at the indicated times 1 h after sensitization with 5 μg/ml anti-TNP-IgE. (top) Immunoblots of PIR-B phosphotyrosine and PIR-B after the precipitation with p91 antibody (sc-9609). (second from top) Immunoblots of PIR-B and SHP-1 after the precipitation with SHP-1 antibody (sc-287). (second from bottom) FcRγ phosphotyrosine and FcRγ after the precipitation with FcRγ antibody (reference 21). (bottom) Antiphosphorylated PLC-γ2 (3871) and PLC-γ2 (3872) immunoblot analysis. (B) The signal intensity of the indicated proteins in A was estimated by densitometric scanning, normalized by the signal intensities of each control protein and represented as a time course after IgE stimulation. Each data point is the mean ± SD of three independent experiments. The signal intensity of B6 BMMCs at times 0 or 0.5 was plotted as 1. Statistical analyses were performed using the Student's *t* test. * (black), $P < 0.05$; or **, $P < 0.01$ between B6 and *B2m*$^{-/-}$ BMMCs. * (blue), $P < 0.05$; or **, $P < 0.01$ between *B2m*$^{-/-}$ and B6 BMMCs. * (red), $P < 0.05$; or **, $P < 0.01$ between *Pirb*$^{-/-}$ and B6 BMMCs. (C) $Ca^{2+}$ mobilization in B6, *B2m*$^{-/-}$, or *Pirb*$^{-/-}$ BMMCs. Intracellular free calcium levels in Indo-1AM–loaded cells were monitored using an LSR system after cells were stimulated with 10 ng/ml TNP-OVA 1 h after sensitization with anti-TNP–IgE. The results are representative of three separate experiments.

interactions between PIR-B and MHC class I in vivo. However, these findings showed that PIR-B on mast cells regulates allergic reaction in vivo.

## DISCUSSION

The increased incidence of allergic diseases, such as atopic dermatitis and bronchial asthma, has become a serious problem to be urgently solved. Although it is well known that combinations of various environmental factors and our genetic elements are related to the development of allergic disorders, clarifying the involvement of genetic factors like MHC in the development of allergy remains highly complicated (41). Recent basic studies have become especially active in the field of inhibitory receptors that can evoke a negative feedback signaling into mast cells (7). On the other hand, it is well accepted that MHC class I molecules expressed ubiquitously are recognized by inhibitory NK receptors (27, 29). Our previous study, however, showed that PIR-B expressed on B cells and myeloid lineage cells can also bind MHC class I as its ligand (25). Human PIR-B relatives

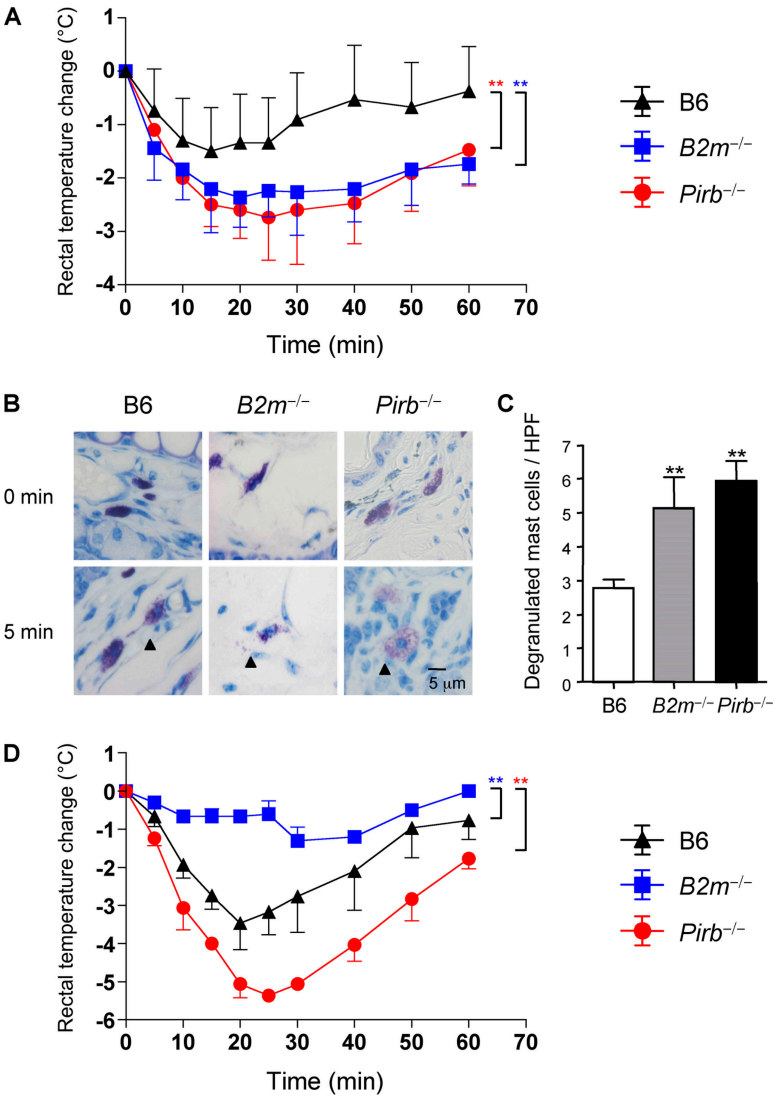


**Figure 8. Augmented IgE-mediated systemic anaphylaxis in *Pirb*$^{-/-}$ or *B2m*$^{-/-}$ mice.** (A) Changes in the rectal temperature of mice during IgE-induced systemic anaphylaxis. B6, *B2m*$^{-/-}$, or *Pirb*$^{-/-}$ mice intravenously received 1 mg TNP-OVA 24 h after administration with anti-TNP-IgE. The monitoring of rectal temperature was started at the time of antigen injection. Data are representative of two separate experiments and are expressed as mean ± SD ($n = 4$). Statistical analyses were performed using two-way analysis of variance. * (blue), $P < 0.01$ between *B2m*$^{-/-}$ and B6 mice. * (red), $P < 0.01$ between *Pirb*$^{-/-}$ and B6 mice. (B) Ear sections were stained with Toluidine blue 5 min after induction of anaphylaxis. Arrows indicate degranulated mast cells. (C) Quantification of degranulated mast cells in tissue sections from ears 5 min after induction of anaphylaxis. Data are shown as mean ± SD. **, $P < 0.01$ between *Pirb*$^{-/-}$ or *B2m*$^{-/-}$ and B6 mice. (D) Mast cell–deficient *W/W*$^{v}$ mice were reconstituted with B6, *B2m*$^{-/-}$, or *Pirb*$^{-/-}$ BMMCs. Systemic anaphylaxis was induced in each mice 16 wk after the reconstitution. Data are representative of two separate experiments and are expressed as mean ± SD ($n = 4$). Statistical analyses were performed using two-way analysis of variance. * (blue), $P < 0.01$ between *W/W*$^{v}$ mice reconstituted with *B2m*$^{-/-}$ and B6 BMMCs. * (red), $P < 0.01$ between *W/W*$^{v}$ mice reconstituted with *Pirb*$^{-/-}$ and B6 BMMCs.

or orthologues, LILRs, are also expressed on myeloid cells (14, 42, 43). Particularly, the amino acid sequences of LILRB1/B2/B3 and PIR-B show almost similar homologies (49.4, 47.3, and 54%, respectively). However, LILRB1 and LILRB2 but not LILRB3 bind MHC class I (14). Moreover, LILRB1 is not expressed on basophils (13). Thus, in the present study, we investigated how an inhibitory MHC class I receptor, human LILRB2 or mouse PIR-B, associates with MHC class I on human basophils or mouse mast cells, respectively. In addition, although LILRB2 was reported to inhibit the basophil activation stimulated with IgE (13), the physiological function of PIR-B in allergic responses remains to be clarified. Therefore, we also examined whether PIR-B has a substantial effect on mast cells. Our present observations, in which primary *Pirb*$^{-/-}$ BMMCs stimulated with IgE were highly activated, reveal a novel inhibitory role of PIR-B in

the mast cell activation. Moreover, we found that *B2m*$^{-/-}$ mice, which lack the expression of PIR-B ligand, MHC class I, also showed augmented in vitro and in vivo IgE-mediated allergic reactions. The FcεRI-mediated signal transductions, including $Ca^{2+}$ influx, were remarkably accelerated in either *B2m*$^{-/-}$ or *Pirb*$^{-/-}$ BMMCs. These results provide a novel insight into how MHC class I itself and its inhibitory receptor dampen the cellular activation triggered by activating receptors on mast cells.

In the present study, we used FRET analyses to show that LILRB2 or PIR-B associate with MHC class I on the same cell surface. Particularly, the constitutive cis interaction between PIR-B and MHC class I could constantly deliver the inhibitory signaling into the mast cells. Supporting this notion, PIR-B on B6 BMMCs was phosphorylated without any stimulation. In addition, the phosphorylation status of PIR-B was down-regulated in *B2m*$^{-/-}$ BMMCs. These findings indicate that deletion of the cis interaction results in a reduction of the constitutive inhibitory signaling through PIR-B, thus prompting the augmented effector responses in either *B2m*$^{-/-}$ or *Pirb*$^{-/-}$ BMMCs. The cis interaction between an inhibitory MHC class I receptor and MHC class I is also observed in NK cells (33). The inhibitory Ly49A NK cell receptor, which contains ITIMs in its cytoplasmic portion, not only binds to the H-2D$^{d}$ ligand expressed on target cells (trans interaction) but also interacts with H-2D$^{d}$ on the same cell surface (cis interaction). The cis interaction represses the binding capacity of Ly49A to H-2D$^{d}$ on target cells, leading to a reduction in the negative signaling mediated by Ly49A. Although it remains unclear how the cis or trans interaction affects the inhibitory signaling by Ly49A, it is possible that the cis interaction dampens the activation threshold of NK cells (33, 44). In contrast, the present observation in which either *B2m*$^{-/-}$ or *Pirb*$^{-/-}$ BMMCs were hypersensitive to IgE stimulation suggests that the PIR-B–MHC class I interaction in cis up-regulates the activation threshold of mast cells. Our previous study demonstrated that PIR-B binds to MHC class I without any allele specificity (25). In addition, LILRs can recognize various classical and nonclassical MHC class I molecules (11, 14, 32, 43). Unlike inhibitory MHC class I receptors on NK cells, it is likely that the cis interaction between LILRB2 or PIR-B and MHC class I delivers self-regulatory signaling and maintains an adequate threshold for cellular activation.

Our present study of the mixed culture of *B2m*$^{-/-}$ BMMCs with B6 or *Pirb*$^{-/-}$ BMMCs showed that PIR-B associates with MHC class I predominantly in cis but not appreciably in trans. However, we cannot exclude the possible occurrence of trans interaction between LILRB2 or PIR-B on one cell surface and MHC class I molecules on the other cell surface. Rather, it is conceivable that LILRB2 or PIR-B can interact with MHC class I both in cis and in trans. In fact, the crystal structure of the LILRB1 and HLA-A2 complexes suggests that LILRB1 can bind to HLA-A2 in trans (45), rationalizing a possible trans interaction between MHC class I and LILRB2 or PIR-B. Our present analytical system using confocal microscopy is only able to depict the cis interactions on a KU812 cell or a mast cell. Although further analysis is required to unequivocally demonstrate that LILRB2 or PIR-B can also bind to MHC class I on other cells in trans, DCs that show increased LILRB2/B3 expression can anergize alloreactive CD4$^{+}$ T cells, suggesting the trans interaction between LILRB2 and MHC class I (46). In addition, the present study did not prove whether PIR-B interacts with MHC class I in trans in vivo, because transferred *B2m*$^{-/-}$ BMMCs failed to be reconstituted. However, our previous study already suggested the possibility of trans interaction between PIRs on DCs and MHC class I molecules on allogeneic T cells in vivo based on observations in which *Pirb*$^{-/-}$ DCs activated alloreactive CD4$^{+}$ and CD8$^{+}$ T cells during the induction of graft-versus-host disease (25). Therefore, it is reasonable to speculate that mast cells or basophils could also recognize MHC class I expressed on surrounding cells in the periphery.

Our present data showed that *B2m*$^{-/-}$ BMMCs mounted augmented effector responses as compared with B6 BMMCs. However, *B2m*$^{-/-}$ BMMCs were slightly less sensitive to IgE stimulation than *Pirb*$^{-/-}$ BMMCs. Supporting this finding, the phosphorylation status of PIR-B was not completely diminished in *B2m*$^{-/-}$ BMMCs. Others also reported a similar observation in which the level of PIR-B tyrosine phosphorylation was reduced by ∼50% in *B2m*$^{-/-}$ mice (47). Recently, a human misfolded MHC class I, HLA-B27 heavy chain dimer was identified as a novel ligand for both PIR-A and PIR-B (48). It has already been reported that the MHC class I heavy chain dimer can be expressed on the cell surface of mouse *B2m*$^{-/-}$ cells (37, 38), as was also observed in our results (Fig. 3 A). Although we do not exclude the possibility of the presence of other ligands expressed on *B2m*$^{-/-}$ mast cells, PIR-B may bind the MHC class I heavy chain dimer on *B2m*$^{-/-}$ cells, resulting in the slight phosphorylation of PIR-B.

In summary, our present study provides evidence that LILRB2 or PIR-B associate with MHC class I in cis and, in particular, that the cis association between PIR-B and MHC class I constitutively delivers negative signaling into mast cells and regulates the cellular activation induced by IgE. This inhibitory regulation through the cis recognition of "self" could be a novel mechanism to maintain adequate cellular responses. Indeed, the deletion of PIR-B also renders other immune cells, such as neutrophils, macrophages, and DCs, sensitive to a variety of activating agents (49, 50).

It is well known that MHC haplotypes relate to the development of various immune disorders, including allergy and autoimmunity. The inhibitory MHC class I receptors—PIR-B in mice and LILRBs in humans—could therefore be potential therapeutic targets that overcome MHC haplotype variations.

## MATERIALS AND METHODS

**Mice.** C57BL/6 (B6) mice were purchased from Charles River Laboratories. *B2m*$^{-/-}$ mice were purchased from the Jackson Laboratory. Mast cell–deficient WBB6F$_1$-*Kit*$^{W}$/*Kit*$^{W\text{-}v}$ (*W*/*W*$^{v}$) mice were purchased from Japan SLC, Inc. *Pirb*$^{-/-}$ 129/B6 mice (34) and *Fcgr2b*$^{-/-}$ 129/B6 mice (8)

were backcrossed onto B6 for 12 generations. Mice were kept and bred in the Animal Unit of the Institute of Development, Aging and Cancer (IDAC) at Tohoku University, an environmentally controlled and specific pathogen-free facility, according to the guidelines for experimental animals defined by the facility. Animal protocols were reviewed and approved by the IDAC Animal Studies Committee. All experiments were performed on 8–12-wk-old age-matched mice.

**Flow cytometry.** KU812 cells, a human early basophilic leukocyte cell line, were donated by M. Numazaki (Tohoku University, Sendai-shi, Japan), and are cultured in $T_{25}$ tissue culture flasks under IL-4–conditioned medium (51, 52). BMMCs were prepared as previously described (36). For flow cytometric analysis of KU812 cells, the following human-specific mAbs were used: anti-FcεRI (CRA1; Kyokuto Pharmaceutical Indust. Co. Ltd.), biotinylated mouse IgG2b (MPC-11; BD Biosciences), anti-LILRB1 (GHI/75; BD Biosciences), anti-LILRB2 (287219; R&D Systems), anti-LILRB3 (222821; R&D Systems), PC5-conjugated anti-LILRB4 (ZM3.8; Beckman Coulter), PC5-conjugated mouse IgG1 (679.1Mc7; Beckman Coulter), anti–HLA-A, B, C (G46-2.6), anti-$\beta_2$m (TÜ99; BD Biosciences), and biotinylated mouse IgM (G155-228; BD Biosciences). The nonlabeled mAbs were biotinylated by using reagents (EZ-Link Sulfo-NHS-Biotin; Pierce Chemical Co.) and labeled with streptavidin–Alexa Fluor 546 (Invitrogen). For flow cytometric analysis of BMMCs, the following mouse-specific mAbs were used: FITC- or PE-conjugated anti–c-Kit (2B8), anti-IgE (R35-72), anti–IL-3α (5B11), anti–H-2D$^b$ (28-17-8), anti–H-2K$^b$/D$^b$ (28-8-6), anti–PIR-A/B (6C1), rat IgG1k (R3-34), rat IgG2a (R35-95), and anti-SIRP1α (P84). These antibodies were all purchased from BD Biosciences. For the detection of MHC class I heavy chain dimer, anti–mouse H-2D$^b$ (B22-249.R1; Cedarlane Laboratories Ltd.) labeled with Alexa Fluor 546 was used (37, 38). Cell surfaces were stained using standard techniques, and flow cytometric analysis was performed using a FACS LSR and CellQuest software (both from BD Biosciences).

**Confocal microscopy analysis.** Confocal laser scanning microscopy of KU812 cells was performed with Alexa Fluor 546–conjugated anti-LILRB2 (287219), LILRB3 (222821), anti-$\beta_2$m (TÜ99), and Alexa Fluor 647–conjugated anti–HLA-A, B, C (G46-2.6). Confocal laser scanning microscopy of BMMCs was performed with Alexa Fluor 488, 546, or 594–conjugated (all from Invitrogen) anti–PIR-A/B (6C1; a gift from H. Kubagawa and M.D. Cooper, University of Alabama at Birmingham, Birmingham, AL), anti–H-2K$^b$/D$^b$ (28-8-6), anti–mouse $\beta_2$m (S19.8; BD Biosciences), and anti–SHPS-1 mAbs (BD Biosciences) after fixing with 4% paraformaldehyde. All of these mAbs were directly labeled by an Alexa Fluor 488, 546, or 647 monoclonal labeling kit (Invitrogen). Alexa Fluor 488, 546, or 594–positive signals were collected by a confocal laser scanning microscope (Fluoview FV1000; Olympus).

**Linearization analysis and the calculation of correlation coefficient.** Linearization analysis determines the location of the receptors observed in one plane of the cell versus the entire cell. Scans of the cell surface were made by drawing a ring-shaped area at the mid focal plane of each cell. The fluorescence intensity of the two target molecules was normalized relative to the highest peak (y axis). The correlation coefficient was calculated on a pixel-by-pixel basis according to

$$\sigma_{x,y} = \sum (x - \bar{x})(y - \bar{x}) \Big/ \sqrt{(x - \bar{x})^2 (y - \bar{y})^2}$$

where $x$ and $y$ are the intensities of the green and red channels in a pixel, and $\bar{x}$ and $\bar{y}$ are the average intensities of the green and red channels within the region of interest. The correlation coefficient theoretically ranges from −1 to 1, where 1 indicates perfect overlap, 0 indicates random distribution, and −1 indicates avoidance.

**FRET analysis and image processing.** KU812 cells or BMMCs plated on poly–L-lysine–coated glass-bottom dishes (Matsunami Glass Ind. Ltd.) were imaged with a Fluoview FV1000 confocal microscopy equipped with three photomultipliers (PMTs), a heated-stage $CO_2$ chamber system, and an objective heater (Olympus) and controlled by FV-10ASW software (Olympus). All imaging of living cells was done at 37°C. An oil-immersion objective (PlanApoN 60; Olympus) was used exclusively for image acquisition. Alexa Fluor 546/647 FRET imaging was performed with sequential excitation at 543 nm and collection of donor–Alexa Fluor 546 (excitation = 555 nm; emission = 625 nm) and FRET (>650 nm) emission, followed by a 633-nm excitation and acceptor–Alexa Fluor 647 (>650 nm) detection. Settings were kept unchanged for analysis of all samples. Unless otherwise indicated in the figure legends, donor emission was detected on the PMT2, and acceptor and FRET emissions were recorded on the PMT3. To determine the donor and acceptor spectral bleed throughs in the FRET setting, individual donor- or acceptor-stained samples were also imaged. After image acquisition, FRET images were calculated using FV-10ASW software and ImageJ software (National Institutes of Health) with the plug-in program PixFRET (available at http://www.unil.ch/cig/page16989.html) (53). The calculated FRET efficiency ($E$) was as follows: $E = 1 - I^{DA}/I^{D}$, where $I^{DA}$ indicates the fluorescence intensity of prebleach donor cells and $I^{D}$ indicates the fluorescence intensity of postbleach donor cells. $E > 0.05$ was defined as the threshold level for substantial transfer efficiency.

**Histamine and cytokine ELISA.** $2 \times 10^6$ BMMCs/well were cultured in 96-well flat plates (BD Biosciences). The supernatants of 12-h cultured BMMCs stimulated with TNP-OVA 1 h after sensitization with 5 μg/ml anti-TNP–IgE (C38-2; BD Biosciences) or LPS (Sigma-Aldrich) were collected and kept frozen at −80°C. The amount of cytokine production was determined by a Multiplex suspension array system (Bio-Rad Laboratories) for MIP-1α, GM-CSF, IL-1β, and IL-6. For histamine release, histamine in the supernatant and cellular pellet fractions was measured by ELISA (Neogen Corporation). The percentage of histamine release was quantitated by the following equation: histamine in supernatant/(histamine in supernatant + histamine in pellet) × 100. For the co-culture experiment, $4 \times 10^6$ mixed BMMCs/well were cultured in 96-well round plates (BD Biosciences) for 12 h. IL-6 concentration in the supernatant of 12-h cultured BMMCs was stimulated with TNP-OVA 1 h after the sensitization with 5 μg/ml anti-TNP–IgE (C38-2; BD Biosciences) and measured by ELISA (BioLegend, Inc.).

**Immunoblot and immunoprecipitation analysis.** $2 \times 10^6$ BMMCs in 1 ml PBS were stimulated for 0 s, 30 s, 2 min, and 30 min at 37°C with 10 ng/ml TNP 1 h after incubation with 5 μg/ml anti-TNP–IgE. Cells were solubilized in a lysis buffer (0.75% Briji-97 [Sigma-Aldrich], 150 mM Hepes [pH 7.4], and 50 mM NaCl) containing 2 mM sodium vanadate (Sigma-Aldrich) and supplemented with proteinase inhibitors (Sigma-Aldrich). For immunoblot analysis, cell lysates were separated by SDS–PAGE gel, transferred to a polyvinylidene difluoride membrane, and detected by antiphosphorylated PLC-γ2 (3871; Cell Signaling Technology, Inc.) and horseradish peroxidase (HRP)–goat anti–rabbit IgG (GE Healthcare). For immunoprecipitation analysis, precleared lysates were sequentially incubated with anti-p91 (sc-9609; Santa Cruz Biotechnology Inc.), anti–SHP-1 (sc-287; Santa Cruz Biotechnology Inc.), or rabbit anti-FcR common γ (polyclonal rabbit IgG) (21) and protein G–conjugated sepharose 4B (GE Healthcare). The immunoprecipitates were separated by SDS-PAGE gel, transferred to a polyvinylidene difluoride membrane, and detected by HRP-antiphosphotyrosine mAb (4G10; Upstate Biotechnology) with the electrochemiluminescence system (GE Healthcare). The detected membranes were stripped off with a stripping buffer that contained 62.5 mM Tris (pH 6.8), 100 mM 2-mercaptoethanol, and 2% SDS and reblotted with the appropriate antibodies. These were anti–PLC-γ2 (3872; Cell Signaling Technology, Inc.), anti-p91, anti–SHP-1, or anti-FcRγ and HRP–goat anti–rabbit IgG (GE Healthcare).

**Measurement of intracellular calcium.** BMMCs were resuspended to $10^7$ cells/ml in RPMI 1640 containing 1% FBS 1 h after incubation with 5 μg/ml anti-TNP–IgE (C38-2). Indo-1AM (Dojindo Laboratories) was

added at a final concentration of 5 mM, and the cells were incubated for a further 30 min. The cells were centrifuged and resuspended in RPMI 1640 at $10^6$ cells/ml. The cells were stimulated with 10 ng/ml TNP-OVA, and the fluorescence intensity of intracellular Indo-1AM was monitored and analyzed using an LSR system.

**Induction of passive systemic anaphylaxis.** Mouse IgE anti-TNP mAbs (C38-2) were administered intravenously through the tail vein in a volume of 200 μl per mouse. Mice were injected intravenously with 1 mg TNP-OVA in PBS 24 h after the injection of IgE (20 μg per mouse). Changes in the core body temperature associated with systemic anaphylaxis were monitored by measuring changes in rectal temperature using a rectal probe coupled to a digital thermometer (Natsume Seisakusyo). For the reconstitution of BMMCs in $W/W^v$ mice, $5\times 10^6$ BMMCs in 100 μl were injected intravenously through the tail vein into $W/W^v$ mice. Mice were housed for 16 wk before the induction of anaphylaxis.

**Histological study.** Mice were killed by cervical dislocation. Their tissues were removed and fixed in 10% (vol/vol) neutral-buffered formalin and embedded in paraffin. The specimens were sectioned at 3 μm and stained with toluidine blue (pH 4). For evaluation of degranulated mast cells, seven high power fields (40× objective) of each ear were examined on a microscope (BX50; Olympus).

**Statistical analysis.** Statistical differences were calculated using the Student's *t* test or two-way analysis of variance. $P < 0.05$ was considered significant.

This work was supported by the Core Research for Evolutional Science and Technology program of the Japan Science and Technology Agency, a grant-in-aid from the Ministry of Education, Culture, Sports, Science and Technology of Japan, and grants from the Mochida Memorial Foundation for Medical and Pharmaceutical Research, the Kanzawa Medical Research Foundation, the Naito Foundation, the Takeda Science Foundation, and the 21st Century Center of Excellence program "Center for Innovative Therapeutic Development Towards the Conquest of Signal Transduction Diseases".

The authors declare that they have no competing financial interests.

**Submitted: 22 March 2006**
**Accepted: 13 March 2007**

## REFERENCES

1. Kawakami, T., and S.J. Galli. 2002. Regulation of mast-cell and basophil function and survival by IgE. *Nat. Rev. Immunol.* 2:773–786.
2. Marshall, J.S. 2004. Mast-cell responses to pathogens. *Nat. Rev. Immunol.* 4:787–799.
3. Gibbs, B.F. 2005. Human basophils as effectors and immunomodulators of allergic inflammation and innate immunity. *Clin. Exp. Med.* 5:43–49.
4. Galli, S.J., S. Nakae, and M. Tsai. 2005. Mast cells in the development of adaptive immune responses. *Nat. Immunol.* 6:135–143.
5. Kinet, J.P. 1999. The high-affinity IgE receptor (FcεRI): from physiology to pathology. *Annu. Rev. Immunol.* 17:931–972.
6. Asai, K., J. Kitaura, Y. Kawakami, N. Yamagata, M. Tsai, D.P. Carbone, F.T. Liu, S.J. Galli, and T. Kawakami. 2001. Regulation of mast cell survival by IgE. *Immunity.* 14:791–800.
7. Katz, H.R. 2002. Inhibitory receptors and allergy. *Curr. Opin. Immunol.* 14:698–704.
8. Takai, T., M. Ono, M. Hikida, H. Ohmori, and J.V. Ravetch. 1996. Augmented humoral and anaphylactic responses in FcγRIIB-deficient mice. *Nature.* 379:346–349.
9. Licht, A., I. Pecht, and R. Schweitzer-Stenner. 2005. Regulation of mast cells' secretory response by co-clustering the type 1 Fcε receptor with the mast cell function-associated antigen. *Eur. J. Immunol.* 35:1621–1633.
10. Daheshia, M., D.S. Friend, M.J. Grusby, K.F. Austen, and H.R. Katz. 2001. Increased severity of local and systemic anaphylactic reactions in gp49B1-deficient mice. *J. Exp. Med.* 194:227–234.
11. Colonna, M., H. Nakajima, F. Navarro, and M. Lopez-Botet. 1999. A novel family of Ig-like receptors for HLA class I molecules that modulate function of lymphoid and myeloid cells. *J. Leukoc. Biol.* 66:375–381.
12. Colonna, M., H. Nakajima, and M. Cella. 2000. A family of inhibitory and activating Ig-like receptors that modulate function of lymphoid and myeloid cells. *Semin. Immunol.* 12:121–127.
13. Sloane, D.E., N. Tedla, M. Awoniyi, D.W. Macglashan Jr., L. Borges, K.F. Austen, and J.P. Arm. 2004. Leukocyte immunoglobulin-like receptors: novel innate receptors for human basophil activation and inhibition. *Blood.* 104:2832–2839.
14. Brown, D., J. Trowsdale, and R. Allen. 2004. The LILR family: modulators of innate and adaptive immune pathways in health and disease. *Tissue Antigens.* 64:215–225.
15. Hayami, K., D. Fukuta, Y. Nishikawa, Y. Yamashita, M. Inui, Y. Ohyama, M. Hikida, H. Ohmori, and T. Takai. 1997. Molecular cloning of a novel murine cell-surface glycoprotein homologous to killer cell inhibitory receptors. *J. Biol. Chem.* 272:7320–7327.
16. Kubagawa, H., P.D. Burrows, and M.D. Cooper. 1997. A novel pair of immunoglobulin-like receptors expressed by B cells and myeloid cells. *Proc. Natl. Acad. Sci. USA.* 94:5261–5266.
17. Yamashita, Y., D. Fukuta, A. Tsuji, A. Nagabukuro, Y. Matsuda, Y. Nishikawa, Y. Ohyama, H. Ohmori, M. Ono, and T. Takai. 1998. Genomic structures and chromosomal location of p91, a novel murine regulatory receptor family. *J. Biochem. (Tokyo).* 123:358–368.
18. Kubagawa, H., C.C. Chen, L.H. Ho, T.S. Shimada, L. Gartland, C. Mashburn, T. Uehara, J.V. Ravetch, and M.D. Cooper. 1999. Biochemical nature and cellular distribution of the paired immunoglobulin-like receptors, PIR-A and PIR-B. *J. Exp. Med.* 189:309–318.
19. Maeda, A., M. Kurosaki, and T. Kurosaki. 1998. Paired immunoglobulin-like receptor (PIR)–A is involved in activating mast cells through its association with Fc receptor γ chain. *J. Exp. Med.* 188:991–995.
20. Yamashita, Y., M. Ono, and T. Takai. 1998. Inhibitory and stimulatory functions of paired Ig-like receptor (PIR) family in RBL-2H3 cells. *J. Immunol.* 161:4042–4047.
21. Ono, M., T. Yuasa, C. Ra, and T. Takai. 1999. Stimulatory function of paired immunoglobulin-like receptor-A in mast cell line by associating with subunits common to Fc receptors. *J. Biol. Chem.* 274:30288–30296.
22. Bléry, M., H. Kubagawa, C.C. Chen, F. Vely, M.D. Cooper, and E. Vivier. 1998. The paired Ig-like receptor PIR-B is an inhibitory receptor that recruits the protein-tyrosine phosphatase SHP-1. *Proc. Natl. Acad. Sci. USA.* 95:2446–2451.
23. Maeda, A., M. Kurosaki, M. Ono, T. Takai, and T. Kurosaki. 1998. Requirement of SH2-containing protein tyrosine phosphatases SHP-1 and SHP-2 for paired immunoglobulin-like receptor B (PIR-B)–mediated inhibitory signal. *J. Exp. Med.* 187:1355–1360.
24. Uehara, T., M. Bléry, D.W. Kang, C.C. Chen, L.H. Ho, G.L. Gartland, F.T. Liu, E. Vivier, M.D. Cooper, and H. Kubagawa. 2001. Inhibition of IgE-mediated mast cell activation by the paired Ig-like receptor PIR-B. *J. Clin. Invest.* 108:1041–1050.
25. Nakamura, A., E. Kobayashi, and T. Takai. 2004. Exacerbated graft-versus-host disease in $Pirb^{-/-}$ mice. *Nat. Immunol.* 5:623–629.
26. Kärre, K. 1993. Natural killer cells and the MHC class I pathway of peptide presentation. *Semin. Immunol.* 5:127–145.
27. Parham, P., and K.L. McQueen. 2003. Alloreactive killer cells: hindrance and help for haematopoietic transplants. *Nat. Rev. Immunol.* 3:108–122.
28. Vivier, E., and N. Anfossi. 2004. Inhibitory NK-cell receptors on T cells: witness of the past, actors of the future. *Nat. Rev. Immunol.* 4:190–198.
29. Parham, P. 2005. MHC class I molecules and KIRs in human history, health and survival. *Nat. Rev. Immunol.* 5:201–214.
30. Moretta, L., and A. Moretta. 2004. Killer immunoglobulin-like receptors. *Curr. Opin. Immunol.* 16:626–633.
31. Borrego, F., M. Masilamani, J. Kabat, T.B. Sanni, and J.E. Coligan. 2005. The cell biology of the human natural killer cell CD94/NKG2A inhibitory receptor. *Mol. Immunol.* 42:485–488.
32. Hamerman, J.A., K. Ogasawara, and L.L. Lanier. 2005. NK cells in innate immunity. *Curr. Opin. Immunol.* 17:29–35.

33. Doucey, M.A., L. Scarpellino, J. Zimmer, P. Guillaume, L.F. Luescher, C. Bron, and W. Held. 2004. *Cis* association of Ly49A with MHC class I restricts natural killer cell inhibition. *Nat. Immunol.* 5:328–336.
34. Ujike, A., K. Takeda, A. Nakamura, S. Ebihara, K. Akiyama, and T. Takai. 2002. Impaired dendritic cell maturation and increased $T_H2$ responses in PIR-$B^{-/-}$ mice. *Nat. Immunol.* 3:542–548.
35. Horváth, G., M. Petrás, G. Szentesi, A. Fábián, J.W. Park, G. Vereb, and J. Szöllösi. 2005. Selecting the right fluorophores and flow cytometer for fluorescence resonance energy transfer measurements. *Cytometry A.* 65:148–157.
36. Takai, T., M. Li, D. Sylvestre, R. Clynes, and J.V. Ravetch. 1994. FcRγ chain deletion results in pleiotrophic effector cell defects. *Cell.* 76:519–529.
37. Allen, H., J. Fraser, D. Flyer, S. Calvin, and R. Flavell. 1986. $\beta_2$-microglobulin is not required for cell surface expression of the murine class I histocompatibility antigen H-$2D^b$ or of a truncated H-$2D^b$. *Proc. Natl. Acad. Sci. USA.* 83:7447–7451.
38. Bix, M., and D. Raulet. 1992. Functionally conformed free class I heavy chains exist on the surface of $\beta_2$ microglobulin–negative cells. *J. Exp. Med.* 176:829–834.
39. Kharitonenkov, A., Z. Chen, I. Sures, H. Wang, J. Schilling, and A. Ullrich. 1997. A family of proteins that inhibit signalling through tyrosine kinase receptors. *Nature.* 386:181–186.
40. Ujike, A., Y. Ishikawa, M. Ono, T. Yuasa, T. Yoshino, M. Fukumoto, J.V. Ravetch, and T. Takai. 1999. Modulation of immunoglobulin (Ig) E–mediated systemic anaphylaxis by low-affinity Fc receptors for IgG. *J. Exp. Med.* 189:1573–1579.
41. Cookson, W. 1999. The alliance of genes and environment in asthma and allergy. *Nature.* 402:B5–B11.
42. Colonna, M., F. Navarro, T. Bellon, M. Llano, P. Garcia, J. Samaridis, L. Angman, M. Cella, and M.A. Lopez-Botet. 1997. A common inhibitory receptor for major histocompatibility complex class I molecules on human lymphoid and myelomonocytic cells. *J. Exp. Med.* 186:1809–1818.
43. Colonna, M., J. Samaridis, M. Cella, L. Angman, R.L. Allen, C.A. O'Callaghan, R. Dunbar, G.S. Ogg, V. Cerundolo, and A. Rolink. 1998. Human myelomonocytic cells express an inhibitory receptor for classical and nonclassical MHC class I molecules. *J. Immunol.* 160:3096–3100.
44. Leibson, P.J., and L.R. Pease. 2004. Having it both ways: MHC recognition in *cis* and *trans*. *Nat. Immunol.* 5:237–238.
45. Willcox, B.E., L.M. Thomas, and P.J. Bjorkman. 2003. Crystal structure of HLA-A2 bound to LIR-1, a host and viral major histocompatibility complex receptor. *Nat. Immunol.* 4:913–919.
46. Chang, C.C., R. Ciubotariu, J.S. Manavalan, J. Yuan, A.I. Colovai, F. Piazza, S. Lederman, M. Colonna, R. Cortesini, R. Dalla-Favera, and N. Suciu-Foca. 2002. Tolerization of dendritic cells by $T_S$ cells: the crucial role of inhibitory receptors ILT3 and ILT4. *Nat. Immunol.* 3:237–243.
47. Ho, L.H., T. Uehara, C.C. Chen, H. Kubagawa, and M.D. Cooper. 1999. Constitutive tyrosine phosphorylation of the inhibitory paired Ig-like receptor PIR-B. *Proc. Natl. Acad. Sci. USA.* 96:15086–15090.
48. Kollnberger, S., L.A. Bird, M. Roddis, C. Hacquard-Bouder, H. Kubagawa, H.C. Bodmer, M. Breban, A.I. McMichael, and P. Bowness. 2004. HLA-B27 heavy chain homodimers are expressed in HLA-B27 transgenic rodent models of spondyloarthritis and are ligands for paired Ig-like receptors. *J. Immunol.* 173:1699–1710.
49. Pereira, S., H. Zhang, T. Takai, and C.A. Lowell. 2004. The inhibitory receptor PIR-B negatively regulates neutrophil and macrophage integrin signaling. *J. Immunol.* 173:5757–5765.
50. Zhang, H., F. Meng, C.L. Chu, T. Takai, and C.A. Lowell. 2005. The Src family kinases Hck and Fgr negatively regulate neutrophil and dendritic cell chemokine signaling via PIR-B. *Immunity.* 22:235–246.
51. Hara, T., K. Yamada, and H. Tachibana. 1998. Basophilic differentiation of the human leukemia cell line KU812 upon treatment with interleukin-4. *Biochem. Biophys. Res. Commun.* 247:542–548.
52. Hosoda, M., M. Yamaya, T. Suzuki, N. Yamada, M. Kamanaka, K. Sekizawa, J.H. Butterfield, T. Watanabe, H. Nishimura, and H. Sasaki. 2002. Effects of rhinovirus infection on histamine and cytokine production by cell lines from human mast cells and basophils. *J. Immunol.* 169:1482–1491.
53. Feige, J.N., D. Sage, W. Wahli, B. Desvergne, and L. Gelman. 2005. PixFRET, an ImageJ plug-in for FRET calculation that can accommodate variations in spectral bleed-throughs. *Microsc. Res. Tech.* 68:51–58.